Comparison of Dual-Energy Computed Tomography Pulmonary Angiography-Derived Contrast Enhancement with Standard Dual-Energy Pulmonary Angiography in Diagnosing Subsegmental Pulmonary Embolism: A Prospective Study

Vivek Yadav[1,#]   Manphool Singhal[1,#]   Muniraju Maralakunte[1]   Navneet Sharma[2]   Arun Sharma[1]   Anupam Lal[1]

[1] Department of Radiodiagnosis and Imaging, Postgraduate Institute of Medical Education and Research, Chandigarh, India
[2] Department of Internal Medicine, Postgraduate Institute of Medical Education and Research, Chandigarh, India

Address for correspondence Manphool Singhal, MD, DNB, FICR, FSCCT, FSCMR, Department of Radiodiagnosis and Imaging, Postgraduate Institute of Medical Education and Research, Chandigarh 160012, India (e-mail: drmsinghal@yahoo.com).

Abstract

Objective   In this study, we compare the diagnostic accuracy of dual-energy (DE) computed tomography pulmonary angiography (CTPA) derived contrast enhancement (DECTPA, CTPA images with iodine maps) with standard dual-energy pulmonary angiography (SCTPA) for diagnosis of subsegmental pulmonary embolism in the cases with clinical suspicion of acute pulmonary embolism (APE).

Materials and Methods   We included 50 cases with clinical suspicion of APE that were referred for CTPA. All the patients underwent CTPA in the dual-energy protocol. Two radiologists evaluated the images. The first radiologist interpreted the SCTPA images (vascular images) and the second radiologist interpreted the DECTPA (CTPA images with iodine maps) for findings of APE. We calculated the sensitivity, specificity, and negative predictive value of DECTPA vis-à-vis SCTPA images.

Results   The DECTPA with the advantage of iodine map utilization yielded higher detection of thrombi in peripheral subsegmental arteries (72 vs. 99; $p = -0.001$) as compared to the SCTPA images by identification of 18 new perfusion defects (interquartile range [IQR]: 0–1) that were consistent with APE. Filling defects were identified in 27 (IQR: 0–4) more subsegmental arteries supplying these 18 areas, which were not detected on SCTPA alone. These 18 perfusion defects were identified in 13 cases. In these 13 cases, 4 new cases were diagnosed that were negative on CTPA ($p = -0.125$).

In the evaluation of the APE, sensitivity and specificity were calculated and it was found that DECTPA showed 100% sensitivity and 86% specificity with 100% negative predictive value in the detection of thrombi as compared to the routine CTPA.

Keywords

► acute pulmonary embolism
► CT pulmonary angiography
► dual-energy CT
► iodine maps
► subsegmental pulmonary embolism

# *Both the authors contributed equally to this article and share the first authorship.*

Conclusion DECTPA has higher sensitivity and negative predictive value in the detection of the subsegmental perfusion defect identification as compared to SCTPA.

Introduction

Acute pulmonary embolism (APE) is a common emergency medical condition, and it is a great masquerade of various conditions manifesting with nonspecific symptoms and signs. Despite the diagnostic advances in the medical field, delayed diagnosis of the APE is an important clinical issue, which may progress to sudden cardiac death.[1] Computed tomography pulmonary angiography (CTPA) is the current standard of practice to confirm the presence of pulmonary thromboembolic events.[2,3] On CTPA, acute thromboembolic events are visualized as intraluminal filling defects along the pulmonary arteries with distension of the luminal caliber.[2,3] Massive PE occluding the main pulmonary arteries and its branches is identified accurately on multidetector CT (MDCT) pulmonary angiography; however, the identification of the subsegmental pulmonary arterial thrombus is challenging on MDCT pulmonary angiography. A meta-analysis reported the sensitivity of conventional CTPA to be 85% (95% confidence interval [CI]: 78.5–85.5).[4] It is essential to identify the PE at any level, as survivors with misdiagnosis of initial APE may present with recurrent PE and death, if prompt diagnosis and treatment is not instituted adequately.[1]

Historically, catheter pulmonary angiography was considered the standard modality to confirm APE in conjunction with the ventilation/perfusion scan (V/Q scan). Although the subsegmental arterial thrombosis is reported to be better detected on catheter-based pulmonary angiography, there was only 45% interobserver agreement for detection of isolated subsegmental PE.[5] The advent of the dual-energy CT (DECT) angiography (DECTPA, CTPA images with iodine maps) has resulted in simultaneous assessment of the pulmonary arteries and parenchymal iodine distribution without additional radiation exposure to the subjects as compared to the conventional CTPA.[5] A recent retrospective study has reported incremental benefit of the iodine map at the detection of subsegmental PE.[6] Currently, there is scarcity of prospective reports on the accuracy of the DECTPA in the evaluation of the APE. We aimed to prospectively estimate the diagnostic performance of (DECTPA, CTPA images with iodine maps) versus SCTPA (only vascular maps) in the evaluation of adult subjects suspected with APE.

Materials and Methods

Subjects

This was a prospective observational cross-section analytical study done at a federally funded nonprofit, tertiary care teaching hospital from July 2018 to October 2019. The institutional ethics committee approved the study. Informed consent was obtained from all the participants after explaining the possible additional radiation exposure from the dual-source DECT study. Fifty adult patients were recruited for DECTPA with clinical suspicion of APE. A diagnosis of pulmonary arterial thrombosis was made with CT when complete or partial intraluminal filling defect(s) were seen along the pulmonary arterial tree with or without luminal enlargement or luminal contrast opacification.[7] The clinical information was completed with the available information from medical records. Children and adolescents (younger than 18 years), pregnant women, those with a previous history of contrast reaction, and those who refused to consent for participation were excluded from the study.

Computed Tomography Examination

Data acquisition was done in 128 dual-source, second-generation Siemens Somatom Definition Flash CT scanner (Siemens Healthineers, Erlangen, Germany). The detector configuration for dual-energy was 64×0.6 mm. The first tube (A) was operated at 100 kilovoltage peak (kVp) with a field of view (FOV) of ~50 cm and the second tube (B) was operated at 140 kVp with a FOV of 33 cm. The corresponding voltage milliampere-seconds were assigned automatically by the CARE Dose 4D modulation system (Siemens Medical Solutions). About 80 mL of low osmolar nonionic iodinated contrast iohexol (Omnipaque 300, GE Healthcare, Shanghai, China) was injected by a dual-phase automated power injector with a flow rate of 4 mL/s followed by a saline chase of 20 mL at the same rate. Single-phase CT acquisition was performed in the craniocaudal direction from lung apices to the dome of the diaphragm in the single breath hold. Data acquisition was done using a region of interest (ROI) placed in the pulmonary trunk with an automatic bolus tracking technique (CARE Bolus, Siemens Healthineers). The automatic scan commenced once the threshold reached 100 HU after approximately 6 seconds.

The raw projection data were reconstructed automatically in three image sets: low-energy image set at 100 kVp, high-energy image set at 140 kVp, and a mixed 100:140-kVp average weighted image with a weighting factor of 0.3 (30% image information from the 100-kVp image and 70% information from the 140-kVp image). This mixing ratio could be freely set between 0%, resulting in a pure anatomic image, and 100%, generating a pure blood flow image that displayed only the color-coded segmented lung parenchyma. Postprocessing of the acquired data was done on a dedicated image processing platform, "syngo.via" (version VB10B HF07, Siemens Healthineers). For analysis, the weighted average pulmonary angiogram reconstruction and DECT iodine maps were generated in coronal, sagittal, and axial reformats.

Image Analysis

All CT scans were analyzed at workstations after reconstruction (at "Syngo.via" workstation for CT 128-slice scanner—Somatom Definition Flash) at the monitor with appropriate window settings (lung and mediastinal window). CT data were evaluated by two radiologists independently (MS and AL). Both were blinded to each other's observations and the clinical information sheet. The first radiologist interpreted only the weighted average pulmonary angiogram images (AL) and the second radiologist interpreted the weighted average pulmonary angiogram images and iodine maps (►Fig. 1).

The weighted average pulmonary angiogram (SCTPA) images of the participants were assessed for the presence or absence of intraluminal thrombus, location of the thrombus (lobes/segments), and level of the thrombus (including the main pulmonary artery [MPA], left pulmonary artery [LPA], right pulmonary artery [RPA], lobar, segmental, and subsegmental). All the subjects were evaluated for the abnormalities in iodine maps in the form of peripheral, wedge-shaped perfusion defects characteristic of PE. Iodine maps were analyzed for the location of perfusion defect, the shape of perfusion defect, and absence or presence of perfusion defects in the corresponding area supplied by the thrombosed artery. Each perfusion defect was compared with the corresponding pulmonary angiogram images for further confirmation and analysis of the pulmonary arterial filling defects.

Statistical Analysis

Patient characteristics, imaging features, and radiation dose are presented using numbers and percentages for categorical variables, mean (SD), and range (minimum, maximum) for quantitative variables with normal distribution. The interquartile range (IQR) was calculated for skewed data. The weighted average pulmonary angiogram and iodine map images were analyzed by the chi-squared test (McNemar's test). Comparison of the number of lobes involved in weighted average pulmonary angiogram and iodine map images was done using the Wilcoxon signed rank test. Sensitivity, specificity, positive predictive value, and negative predictive value of weighted average pulmonary angiogram and iodine map images were worked out to SCTPA images and vice versa. A p-value of less than 0.05 was considered statistically significant. All statistical analyses were computed using SPSS software (version 22).

Results

A total of 50 patients, with an equal proportion of both genders (25 each/50%) and a mean age of 46.8 years, participated in the study. Twenty of 50 (42%) patients showed intraluminal filling defects in the pulmonary arterial tree suggestive of APE. Analysis of the weighted average pulmonary angiograms (SCTPA) revealed 116 intraluminal filling defects. Most commonly, the filling defects are noted in the
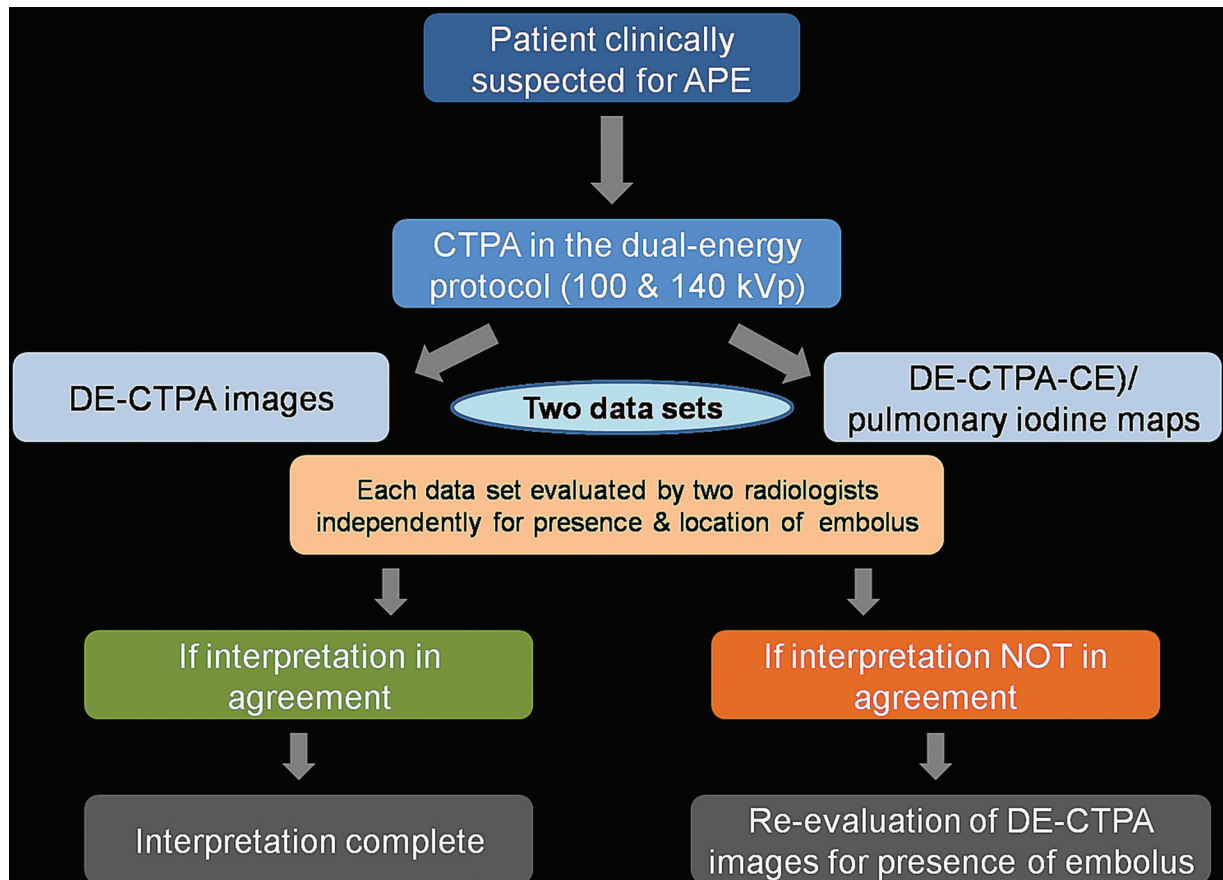

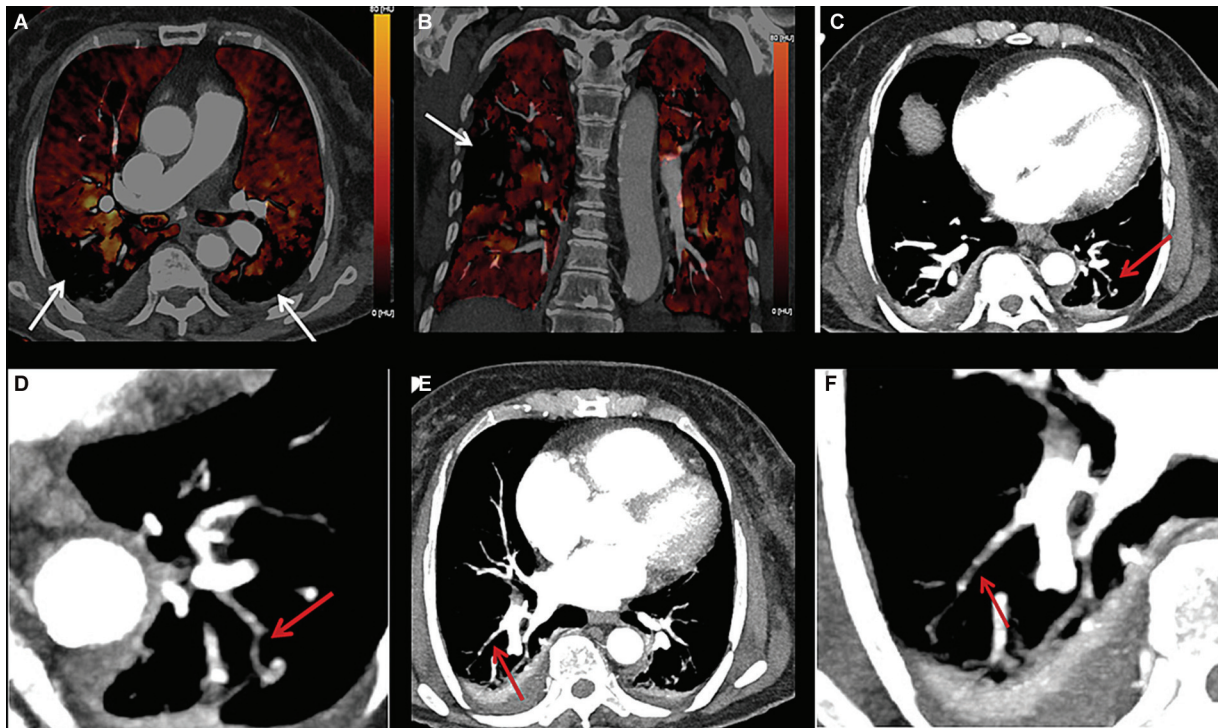**Fig. 1** Flow diagram of the study design.

Fig. 2 A 78-year-old woman with bilateral knee replacement on postoperative day 3 presented with acute onset shortness of breath showed multiple peripheral wedge-shaped areas of perfusion defects (white arrows) in the bilateral lung fields on iodine map (**A**) axial and (**B**) coronal images on dual-energy CT pulmonary angiography (DECTPA). Thrombi are seen in subsegmental arteries (*red arrows*) supplying these areas on (**C,E**) axial and (**D,F**) magnified averaged pulmonary angiogram. These subsegmental thrombi were missed on SCTPA images and detected thereafter after review of DECTPA images (iodine maps and vascular images).

subsegmental pulmonary arteries ($n = 72$ [62%]; IQR: 0–3), followed by segmental pulmonary arteries ($n = 34$ [29.3%]; IQR: 0–1), and with the least common involvement of the MPA and its branches (RPA and LPA) accounting for 10 (8.6%) filling defects.

The DE-derived iodine maps showed wedge-shaped perfusion defects corresponding to APE in 25/50 (50%) patients. The iodine map findings and correlation with average weighted pulmonary angiogram images revealed 143 intraluminal pulmonary arterial defects. The subsegmental pulmonary arteries were the most common sites ($n = 99$

[69.2%]; IQR: 0–4), followed by segmental pulmonary arteries ($n = 34$ [23.8%]; IQR: 0–1), and least common involvement of the MPA and its branches (LPA and RPA) accounting for 7% (10) of total filling defects. The subsegmental pulmonary arterial filling defects were distributed most commonly in the RLL ($n = 18$ [29.5%]) and LLL ($n = 17$ [27.9%]), followed by the right middle lobe (RML) arteries ($n = 12$ [19.6%]), and least common in the right upper lobe (RUL) and left upper lobe (LUL; $n = 7$ [11.5%] each; ►**Figs. 2–4**). Additional 18 new areas of perfusion defects were identified on iodine maps and their correlation with a weighted average pulmonary
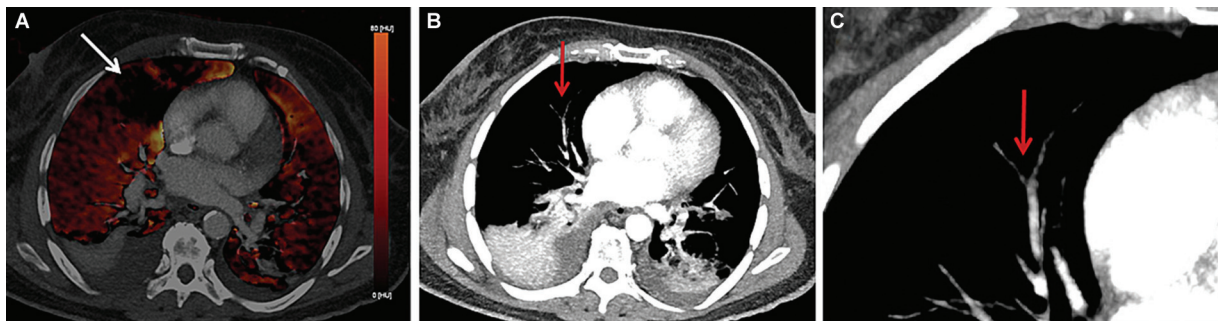

Fig. 3 A 66-year-old woman, a case of carcinoma ovary, presenting with acute onset shortness of breath and hypoxia, showed a subsegmental thrombus in the left lower lobe. On evaluation with dual-energy computed tomography (CT) pulmonary angiography (DECTPA), an additional peripheral wedge-shaped area of perfusion defect (*white arrow*) was seen in the right middle lobe on iodine map in (**A**) the axial image with occlusion of the corresponding subsegmental arteries (*red arrows*) supplying the area seen on (**B**) the axial maximum-intensity projection (MIP) image and better appreciated in (**C**) the magnified axial MIP image on averaged pulmonary angiogram. These subsegmental thrombi were missed on SCTPA images and detected subsequently after review of the DECTPA images (iodine maps and vascular images).
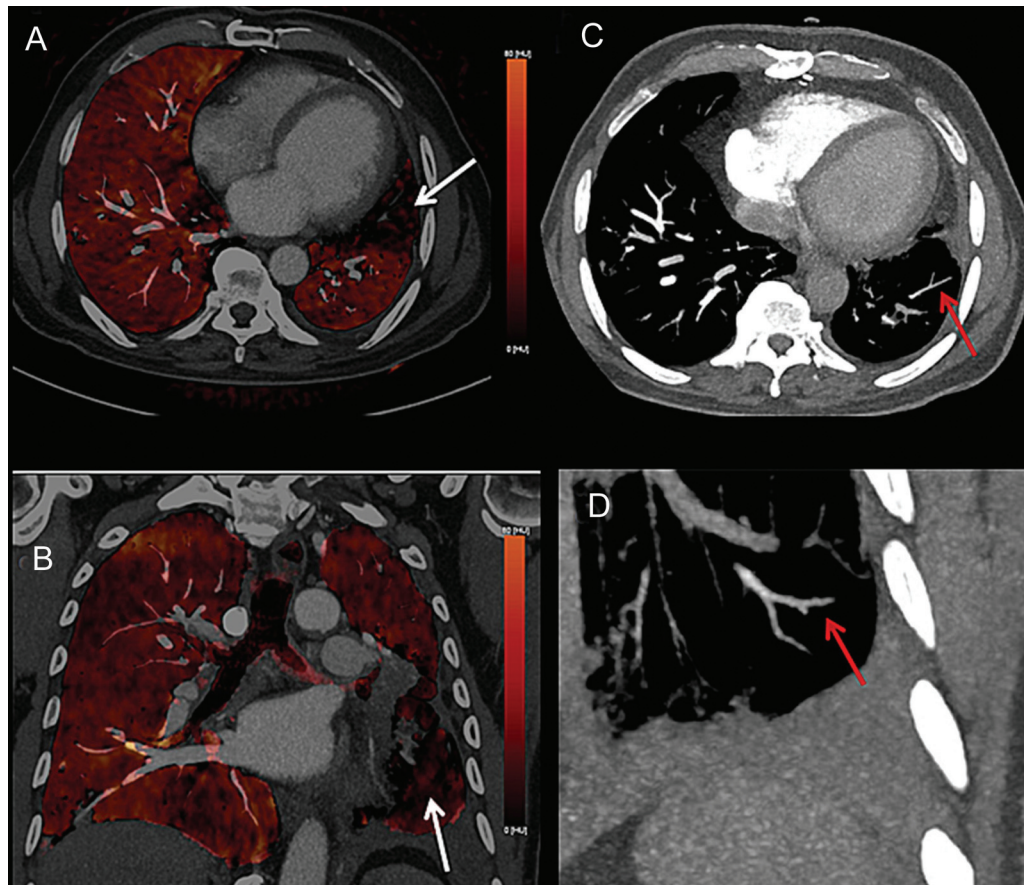
Fig. 4 In a 61-year-old male patient with diagnosis of adenocarcinoma lung (involving ligula), status post operative and radiotherapy presented with acute onset, shortness of breath, a peripheral wedge-shaped area of perfusion defect (white arrows) is seen in left lower lobe on iodine map in axial (**A**) and coronal images (**B**) with occlusion of corresponding subsegmental arteries (red arrows) supplying the area seen on axial MIP image (**C**) and coronal (magnified) MIP image (**D**). These subsegmental thrombi were not detected at first on SCTPA, however after examining the iodine map and subsequent evaluation these thrombi were detected.

angiogram. The additional APE filling defects were signifi-cantly found in the RML subsegmental arteries in seven cases ($p = \sim 0.01$).

Comparison of the Weighted Average Pulmonary Angiogram and Iodine Maps with a Weighted Average Pulmonary Angiogram

The performances of the weighted average pulmonary an-giogram and iodine map analysis (DECTPA) in the identifica-tion of the filling defects and their corresponding perfusion defects were similar in the evaluation of the MPA, LPA, and RPA (10 vs. 10 thrombi) as well as in the lobar and segmental arteries (34 vs. 34 thrombi). The iodine map identified addi-tional 18 new perfusion defects (IQR: 0–1) consistent with PE and 27 (IQR: 0–4) filling defects involving the subsegmental arteries, which were missed on weighted average pulmonary angiogram (SCTPA) alone (►Table 1; ►Figs. 2–4). The addi-tionally detected subsegmental thrombi and perfusion defects were statistically significant with a p-value of 0.01. False-negative defects in pulmonary arteries were found

Table 1 Summary of filling and perfusion defects (iodine map) involving pulmonary arterial tree segments using weighted average pulmonary angiogram (SCTPA) and the combined evaluation of iodine maps with a weighted average pulmonary angiogram (DECTPA)

Pulmonary arterial tree	Filling defects on pulmonary angiogram on SCPTA	Perfusion defects on iodine maps on DECTPA	Extra filling defects on DECTPA	p-Value
Main artery and its branches	10	10	0	1
Lobar and segmental arteries	34	34	0	1
Subsegmental arteries	72	99	27	0.001
Total number of thrombi	116	143	27	0.001

Abbreviation: DECTPA, dual-energy CT pulmonary angiography.

in 4 cases among the 18 perfusion defects in 13 cases, based on sole pulmonary angiogram (SCTPA) analysis, but it was not statistically significant ($p = \sim 0.125$).

These newly diagnosed four cases on DECTPA showed filling defects only in subsegmental arteries. So, in total, 10 (20%) cases had isolated subsegmental thrombi in this study. In six cases of isolated subsegmental thrombi detected on weighted average pulmonary angiogram, three (50%) cases showed new subsegmental thrombi on a combined evaluation of iodine maps and weighted average pulmonary angiograms (DECTPA).

In evaluating the APE, sensitivity and specificity were calculated and it was found that combined evaluation of weighted average pulmonary angiogram with iodine maps analysis (DECTPA) showed 100% sensitivity and 86% specificity with 100% negative predictive value in the detection of thrombi as compared to the weighted average pulmonary angiograms alone. The weighted average pulmonary angiogram results showed 100% specificity and 84% sensitivity with 86% negative predictive value in the identification of the thrombi as compared to iodine maps.

The total radiation exposure in the acquisition of the DECTPA study was recorded in each patient; the mean effective radiation dose was 2.56 mSv (± 0.9).

Discussion

Our study found significant incremental trend at detection of subsegmental PEs on evaluation of iodine maps as compared to the weighted average pulmonary angiogram. We found 27 new subsegmental PEs on iodine map with a *p*-value of 0.01. No new PEs were found at evaluation of the MPA and its branches on iodine maps. A retrospective study on cancer patients with suspicion of APE reported small difference in using DECTPA over conventional angiography in the detection of subsegmental PEs.[6] The authors have reported new PEs in 2.3% of the subjects on iodine maps.[6] A few animal studies have also reported significant increased detection of subsegmental and distal PEs on iodine maps as compared to the pulmonary angiography alone.[8,9] Tang et al reported a sensitivity of 96% for the detection of subsegmental and distal PEs on iodine maps as compared to a sensitivity of 24% on pulmonary angiogram evaluation.[9] We found 100% sensitivity, 100% negative predictive value (NPV), and 86% specificity on iodine maps obtained from DECTPA. The subsegmental and distal PEs may be missed in a significant number of patients by conventional/standard pulmonary angiogram (SCTPA) due to the smaller caliber of the peripheral vessels.

The early literature has reported a controversial role of detection of subsegmental PEs on conventional CT pulmonary angiography with no added benefit to the patient management.[10] However, the recent literature report a good correlation between the burden of perfusion defects on DECTPA and global right ventricular dysfunction.[11–14] A few authors have also concluded that the perfusion defect score may become a promising biomarker for clinical risk stratification of the APE.[11] Apfaltrer et al investigated the prognostic value of perfusion defect volume (PDvol) at

DECTPA and adverse clinical outcome in subjects with APE; and the authors reported significant ($p = 0.002$) adverse events associated with the higher PDvol.[12] A Chinese study reported significant correlation between high CT obstruction index (Qanadli index), oxygen saturation ($r = 0.934$), and pulmonary artery pressure ($r = 0.813$).[13] Yu et al reported the Qanadli index to be an accurate method for distinguishing massive and submassive PE.[13] A retrospective study also reported an association of increased PDvol with right ventricular strain in subjects with PE.[14]

Current evidence states that the higher burden of the pulmonary defects detected on iodine maps of DECTPA may result in accurate severity assessment of subjects with massive PE[11–14]; nevertheless, the presence of isolated subsegmental occlusions in subjects with submassive PE is less understood currently. Further, longitudinal studies evaluating the significance of submassive and subsegmental PEs are warranted to understand the current knowledge gap. It is worth noting that the radiation exposure in the acquisition of DECTPA is either comparable or less (effective radiation dose in the present study was 2.56 mSv ± 0.9 as compared to SCPTA. Authors have reported a mean effective radiation of 3.17 ± 1.2 mSv with SCTPA on dual source CT platform.[15] Considering the benefits derived, DECPTA should be considered wherever possible.

Our study has a few limitations. First, the perfusion defects were not correlated with any CT or other clinical parameters to risk stratify the PEs. Second, the patients with isolated subsegmental PEs were not followed up to know the clinical significance of the pulmonary defects found on iodine maps.

In conclusion, we found a significant incremental trend of detection of subsegmental PEs using iodine maps of DECTPA with 100% NPV. The findings of our study highlight the enhanced diagnostic performance of radiologists at accurate detection of pulmonary thrombosis even in the peripheral lung parenchyma.

Conflict of Interest
None declared.

References

1 Ozsu S, Oztuna F, Bulbul Y, et al. The role of risk factors in delayed diagnosis of pulmonary embolism. Am J Emerg Med 2011;29(01): 26–32

2 Remy-Jardin M, Pistolesi M, Goodman LR, et al. Management of suspected acute pulmonary embolism in the era of CT angiography: a statement from the Fleischner Society. Radiology 2007;245 (02):315–329

3 Patel S, Kazerooni EA. Helical CT for the evaluation of acute pulmonary embolism. AJR Am J Roentgenol 2005;185(01):135–149

4 Hess S, Frary EC, Gerke O, Madsen PH. State-of-the-art imaging in pulmonary embolism: ventilation/perfusion single-photon emission computed tomography versus computed tomography angiography—controversies, results, and recommendations from a systematic review. Semin Thromb Hemost 2016;42 (08):833–845

5 Pontana F, Faivre JB, Remy-Jardin M, et al. Lung perfusion with dual-energy multidetector-row CT (MDCT): feasibility for the evaluation of acute pulmonary embolism in 117 consecutive patients. Acad Radiol 2008;15(12):1494–1504

6 Weidman EK, Plodkowski AJ, Halpenny DF, et al. Dual-energy CT angiography for detection of pulmonary emboli: incremental benefit of iodine maps. Radiology 2018;289(02):546–553

7 Gottschalk A, Stein PD, Goodman LR, Sostman HD. Overview of prospective investigation of pulmonary embolism diagnosis II. Semin Nucl Med 2002;32(03):173–182

8 Zhang LJ, Zhao YE, Wu SY, et al. Pulmonary embolism detection with dual-energy CT: experimental study of dual-source CT in rabbits. Radiology 2009;252(01):61–70

9 Tang CX, Zhang LJ, Han ZH, et al. Dual-energy CT based vascular iodine analysis improves sensitivity for peripheral pulmonary artery thrombus detection: an experimental study in canines. Eur J Radiol 2013;82(12):2270–2278

10 Wiener RS, Schwartz LM, Woloshin S. Time trends in pulmonary embolism in the United States: evidence of overdiagnosis. Arch Intern Med 2011;171(09):831–837

11 Kong WF, Wang YT, Yin LL, Pu H, Tao KY. Clinical risk stratification of acute pulmonary embolism: comparing the usefulness of CTA obstruction score and pulmonary perfusion defect score with dual-energy CT. Int J Cardiovasc Imaging 2017;33(12):2039–2047

12 Apfaltrer P, Bachmann V, Meyer M, et al. Prognostic value of perfusion defect volume at dual energy CTA in patients with pulmonary embolism: correlation with CTA obstruction scores, CT parameters of right ventricular dysfunction and adverse clinical outcome. Eur J Radiol 2012;81(11):3592–3597

13 Yu T, Yuan M, Zhang Q, Shi H, Wang D. Evaluation of computed tomography obstruction index in guiding therapeutic decisions and monitoring percutanous catheter fragmentation in massive pulmonary embolism. J Biomed Res 2011;25(06):431–437

14 Bauer RW, Frellesen C, Renker M, et al. Dual energy CT pulmonary blood volume assessment in acute pulmonary embolism - correlation with D-dimer level, right heart strain and clinical outcome. Eur Radiol 2011;21(09):1914–1921

15 Thakur R, Singhal M, Aggrawal AN, et al. Comparison of high-pitch prospective electrocardiogram-gated pulmonary CT angiography with standard CT pulmonary angiography on dual-source CT for detection of subsegmental pulmonary embolism in patients suspected of acute pulmonary embolism. Pol J Radiol 2022;87(01):e296–e303